ACS OMEGA

Open Access

http://pubs.acs.org/journal/acsodf

Article

Study of MoS_2 as an Electric Field Sensor and the Role of Layer Thickness on the Sensitivity

Mohammad Razzakul Islam,[‖] Jiali Hu,[‖] Afsal Kareekunnan,* Akihiro Kuki, Takeshi Kudo, Takeshi Maruyama, Atsushi Nishizaki, Yuki Tokita, Masashi Akabori, and Hiroshi Mizuta

Cite This: *ACS Omega* 2024, 9, 29751−29755

Read Online

ACCESS | Metrics & More | Article Recommendations

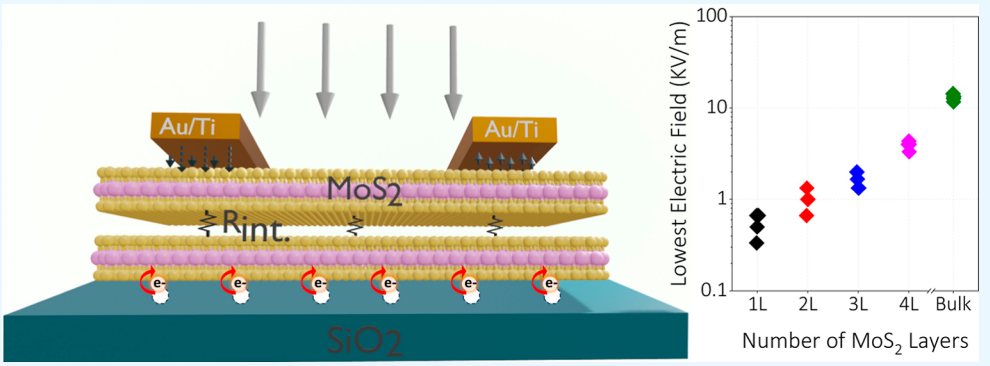

ABSTRACT: In this study, we investigate the scope of molybdenum disulfide (MoS_2) as an electric field sensor. We show that MoS_2 sensors can be used to identify the polarity as well as to detect the magnitude of the electric field. The response of the sensor is recorded as the change in the drain current when the electric field is applied. The sensitivity, defined as the percentage change in the drain current, reveals that it has a linear relation with the magnitude of the electric field. Furthermore, the sensitivity is highly dependent on the layer thickness, with the single-layer device being highly sensitive and the sensitivity decreasing with the thickness. We have also compared the electric field sensitivity of MoS_2 devices to that of previously studied graphene devices and found the former to be exceptionally sensitive than the latter for a given electric field magnitude.

INTRODUCTION

Two-dimensional materials are found to be excellent choices for various sensing applications that have a profound impact on our day-to-day lives.[1−4] However, the use of two-dimensional materials as an electric field sensor has not been extensively studied, although electric field sensors find various real-life applications, including lightning detection. In recent years, graphene was used as an electric field sensor by Wang et al.[5] and our group.[6] While we clarified the mechanism of electric field sensing in two-dimensional material-based sensors,[6] we have also demonstrated that graphene sensors can detect lightning and the changes in the atmospheric electric field, with a detection limit comparable to that of the existing state-of-the-art electric field sensors.[7] As per the mechanism, the response of the sensor, which is measured as the variation in the drain current with the applied electric field, originates from the transfer of charges between the channel and the traps at the SiO_2/channel interface. The sensitivity of the sensor depends on the number of charges transferred. One of the ways to improve the sensitivity is to enhance the carrier mobility, thereby increasing the number of carriers moving through the channel at a given time, which in turn increases the probability of carriers being trapped. Thus, in an effort to improve the carrier mobility, we used hexagonal boron nitride-encapsulated graphene, which showed significant improvement in the sensitivity, owing to the enhanced carrier mobility.[8]

Another approach to improve the sensitivity is to use a material with a high density of states (DOS), as the number of charge carriers participating in the trapping and detrapping process (between the channel and the traps at the channel/SiO_2 interface) is limited by the DOS at the Fermi level. In graphene, the Fermi level is usually near the charge neutrality point (CNP), depending on the amount of external doping.[9−12] However, since the DOS near the CNP in graphene is very small, it is challenging to achieve high sensitivity. Thus, it is necessary to use a material with a high

Received: April 7, 2024
Revised: May 9, 2024
Accepted: June 17, 2024
Published: June 25, 2024

https://doi.org/10.1021/acsomega.4c03350
ACS Omega 2024, 9, 29751−29755

DOS around the Fermi level for better sensitivity. One such material is MoS_2, a widely used two-dimensional transition metal dichalcogenide.[13,14] While MoS_2 has a much higher DOS than graphene,[15] it also has a higher DOS than other commonly used two-dimensional transition metal dichalcogenides such as $MoSe_2$, WS_2, and WSe_2.[16] Thus, in this study, we investigated the prospect of using MoS_2 as an electric field sensor. We also study the effect of layer thickness on electric field sensitivity in detail.

RESULTS AND DISCUSSION

Figure 1a,b shows the schematic diagram and optical micrograph of the MoS_2 device, respectively. The fabrication process is as follows. The MoS_2 flakes are exfoliated from their bulk counterpart on a lightly doped (40−60 Ω·cm) Si/SiO_2 substrate with a SiO_2 thickness of 285 nm. Thin flakes were identified by using an optical microscope. Later, the number of layers was confirmed by using Raman spectroscopy with a 532 nm laser. Figure 1c shows the Raman spectra of 1L, 2L, 3L, 4L, and bulk MoS_2 crystals (here, bulk refers to any number of layers above 4 layers, which are difficult to distinguish using our Raman spectrometer). The number of layers is determined based on the E_{2g}^1 and A_{1g} peak positions and the difference between the two peaks as shown in Figure 1d.[17,18] Once the desired MoS_2 layer thickness was confirmed, the contacts were fabricated by electron beam lithography patterning and subsequent deposition of Ti/Au (15 nm/55 nm) metals by using electron beam evaporation.

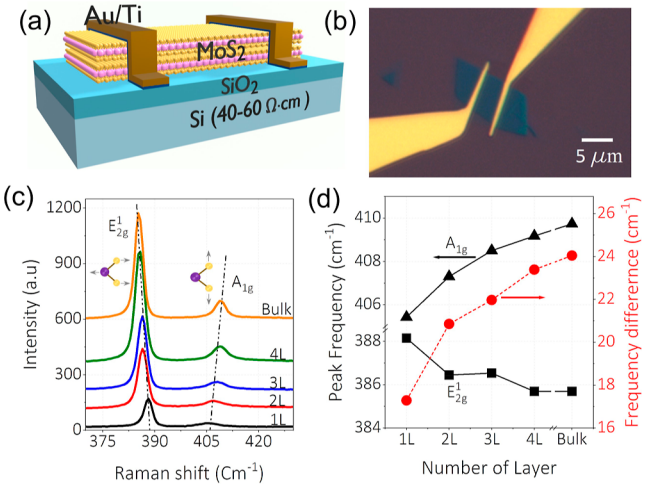

Figure 1. (a) Schematic diagram and (b) optical image of a bilayer MoS_2 electric field sensor. (c) Raman spectra of MoS_2 flakes of different thicknesses showing the E_{2g}^1 and A_{1g} peaks. (d) E_{2g}^1 and A_{1g} peak positions and the difference between the two peaks as a function of the number of MoS_2 layers.

Figure 2a shows the gate characteristics of MoS_2 devices with varying layer thicknesses. For all of the measurements, a source−drain voltage (V_{DS}) of 0.5 V was used. The gate characteristics imply that the MoS_2 channels of all of the devices are n-type. As per previous reports on MoS_2 devices, annealing at a moderate temperature (between 150 and 200 °C) significantly improves the device's performance.[19−22] Thus, the devices were subjected to vacuum annealing at 150 °C for 4 h. The electrical measurements were again performed under vacuum once the temperature was reduced to room temperature. Figure 2b compares the gate characteristics of a single-layer device before and after vacuum annealing. An overall shift toward the positive gate voltage can be seen after annealing. The threshold voltage, V_{TH} (the voltage at which the drain current starts to increase), extracted from the logarithmic plot is also shown in the figure. A shift in V_{TH} from −28 V before annealing to −14 V after annealing implies a reduction in n-doping as a result of vacuum annealing. All of the devices for other thicknesses also followed a similar trend before and after annealing. The reduction in n-doping is attributed to the improved MoS_2/SiO_2 interface and the subsequent transfer of electrons from the channel to the positively charged interface traps.[20] Figure 2c compares the field-induced carrier mobilities of the devices before and after annealing. The error bar is the standard deviation and the dot is the mean of the carrier mobility. The following observations can be made from the plot. (i) Annealing improves the carrier mobility in all devices irrespective of the thickness of the channel. This is because the neutralization of positively charged interface traps due to annealing significantly reduces the Coulomb scattering. (ii) Devices with thin channels (especially single-layer and bilayer devices) show a drastic device-to-device variation in carrier mobility compared to devices with thick channels. (iii) The carrier mobility increases with the increase of the channel thickness. This is in line with the earlier studies which have shown that the single layer MoS_2 has the least mobility owing to the Coulomb scattering from the charged impurities at the SiO_2/channel interface.[23−25] As

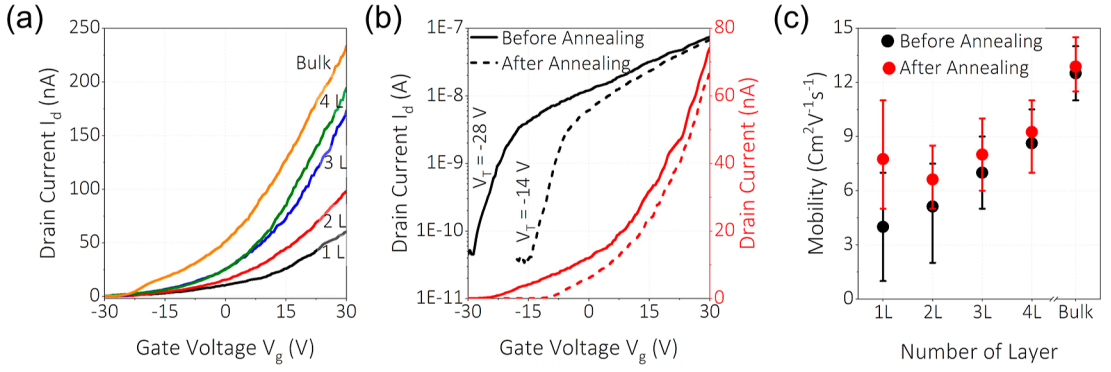

Figure 2. (a) Gate characteristics of the 1L, 2L, 3L, 4L, and bulk MoS_2 devices. The source−drain voltage is 0.5 V. (b) Gate characteristics of monolayer MoS_2 before (black) and after (red) 4 h vacuum annealing at 150 °C. (b) Calculated field effect mobilities of 1L, 2L, 3L, 4L, and bulk MoS_2 devices before and after vacuum annealing.

https://doi.org/10.1021/acsomega.4c03350
ACS Omega 2024, 9, 29751−29755

the number of MoS_2 layers increases, these charged impurities are screened by the bottom layers, thereby increasing the carrier mobility.

Next, we look at the response of these MoS_2 devices in an applied electric field. The measurement setup consists of two parallel plates across which a voltage is applied, with the sensor kept in between them.[6] Both positive and negative voltages in the range of 10 V−5 kV can be applied on the top plate. The bottom plate is kept grounded. The working distance between the two plates is 3 cm. The measurement is performed as follows. The desired electric field is generated across the parallel plates by applying the corresponding voltage on the top plate. The source−drain current measurement is initiated using the Keithley 4200A semiconductor parameter analyzer. This measures the source−drain current with the electric field ON (I_{ON}). In all of the measurements, a source−drain voltage of 0.5 V was used. While the source−drain current is being measured, the electric field across the plates is turned off, whereby, the source−drain current with the electric field OFF (I_{OFF}) is measured. Figure 3a,b shows the response of a single-layer MoS_2 device for positive and negative electric fields, respectively. The magnitude of the applied electric field is 33 kV/m in both cases. It can be seen that the response of the sensor is opposite for positive and negative electric fields. While the drain current increases under a positive electric field, it decreases under a negative electric field. The above observation can be explained based on the mechanism of electric field sensing in two-dimensional materials which lies in the transfer of carriers between the channel and the traps at the SiO_2/channel interface.[6] The direction of charge transfer depends on the polarity of the applied electric field, as dictated by the Coulomb interaction. Under a positive electric field, electrons are detrapped into the channel. In our case, MoS_2 being n-doped, these additional electrons shift the Fermi level up to the high DOS region, resulting in an increase in drain current. Whereas under a negative electric field, the electrons from the channel are trapped into the interface trap states, shifting the Fermi level down toward the low DOS region, resulting in a decrease in drain current.

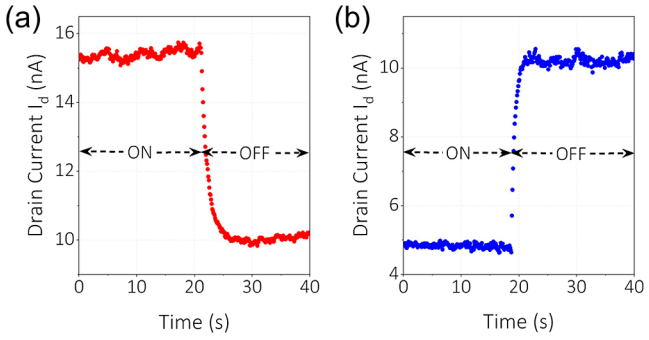

Figure 3. Response of the MoS_2 electric field sensor to (a) positive and (b) negative electric fields. The magnitude of the applied electric field is 33 kV/m.

From the mechanism of electric field sensing, it is evident that the number of carriers trapped/detrapped will be proportional to the strength of the electric field, which will be reflected as the relative change in I_{ON} compared to I_{OFF}. Larger the electric field, the farther I_{ON} will be from I_{OFF}. Thus, it is appropriate to define the sensitivity of the electric field sensor in terms of the percentage change in drain current

$$S_{EF} = \frac{|I_{ON} - I_{OFF}|}{I_{OFF}} \times 100$$

where I_{ON} and I_{OFF} are the drain current measured when the electric field is ON and OFF, respectively. Figure 4a shows the electric field sensitivity of MoS_2 devices of thicknesses 1L, 2L, 3L, 4L, and bulk for different magnitudes of positive and negative electric fields. The error bar is the standard deviation and the dot is the mean electric field sensitivity. The following observations can be made from the plot. (i) As one would anticipate, the sensitivity increases linearly with the electric field strength for devices with varying thicknesses. This is attributed to the increase in the number of carriers trapped/detrapped with the strength of the electric field. (ii) It can be seen that the single-layer MoS_2 device exhibits the highest sensitivity, with the sensitivity consistently reducing with the increase in the number of layers. To explain this, we have to look at two processes happening in the MoS_2 layer during the sensing measurement, which are shown schematically in Figure 4b. One is the charge trapping/detrapping process when the electric field is ON, which happens in the bottom layer close to the oxide (SiO_2) layer. Another is the charge injection to the channel through the source−drain electrodes, which are connected to the top layer.[26] Here, we make an assumption that the charge carriers are predominantly injected into the top layer by the source−drain electrodes. Although the electrodes may make a "side contact" with the edges of the lower layers in a multilayer scenario, any contact area there is much smaller than the contact area at the top layer. Thus, it is reasonable to assume that most of the charge injection occurs in the top layer. For a single-layer MoS_2 device, both processes (trapping/detrapping and charge injection from the source−drain electrodes) happen in the same layer. Whereas for a bilayer MoS_2 device, while the trapping/detrapping happens at the bottom layer, the charge injection happens at the top layer. Thus, the trapped/detrapped charges have to overcome the interlayer resistance (which is estimated to be 2.4 kΩ·μm[27]) between the layers to participate in the charge conduction process, making less trapped/detrapped charges participate in the conduction process.[26−28] Hence, bilayer MoS_2 has less sensitivity than single-layer MoS_2 for the same magnitude of the electric field. In the same way, with every increase in the number of layers, the effective interlayer resistance encountered by the charges increases, reducing the sensitivity. (iii) The lowest electric field detected by the MoS_2 device varies drastically with the thickness of the channel (Figure 4c). While the single-layer device could detect an electric field as low as 333 V/m, the lowest fields detected by 2L, 3L, 4L, and bulk are 667, 1.3, 3.3, and 11.7 kV/m, respectively. This observation is also consistent with the above explanation of the role of interlayer resistance in the electric field sensitivity for the multilayer MoS_2 device, where the charges trapped/detrapped in the bottom layer have to overcome the interlayer resistance to reach the top layer through which the conduction happens predominantly. Consequently, as the number of layers increases, charge carriers require a higher electric field to overcome the interlayer resistance, thereby increasing the magnitude of the detectable lowest electric field.

We have also measured the sensitivity of the MoS_2 electric field sensor after annealing and compared it to the performance of the sensor before annealing for a single-layer device as shown in Figure 4d. The error bar is the standard deviation and the dot is the mean electric field sensitivity. It can be seen

https://doi.org/10.1021/acsomega.4c03350
ACS Omega 2024, 9, 29751−29755

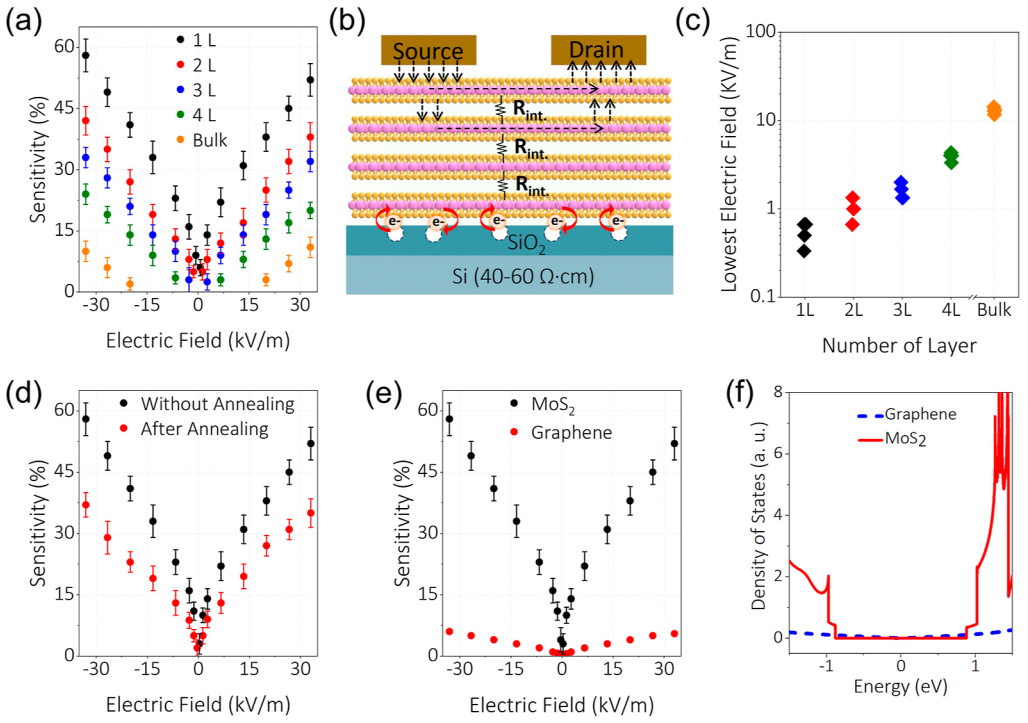

Figure 4. (a) Electric field sensitivity of MoS_2 devices with different thicknesses for both positive and negative electric fields. (b) Schematic diagram showing the mechanism of electric field sensing in MoS_2. (c) Minimum electric field detected as a function of the number of MoS_2 layers. (d) Comparison of electric field sensitivity of the single-layer MoS_2 device before (black) and after (red) vacuum annealing. (e) Comparison of electric field sensitivity of the single-layer MoS_2 device to that of a single-layer graphene device. (f) Comparison of DOS of single-layer MoS_2 and graphene devices.

that the sensitivity decreased after annealing. This is true for all of the devices of different thicknesses. The decline in sensitivity following annealing can be explained based on the variation in the doping concentration post annealing as seen in Figure 2b. As discussed earlier, as a consequence of annealing, a clean channel/oxide interface facilitates the transfer of electrons to the positively charged traps at the interface, neutralizing them.[20] This leads to two interconnected phenomena. First, the neutralization of traps decreases trap density, subsequently reducing electric field sensitivity, as the sensitivity depends on the number of charge carriers transferred between the MoS_2 channel and the traps. Second, after annealing, there is a change in the doping level in the channel after electron transfer to the positively charged traps (as depicted in 2b, where the V_{TH} shifts toward positive gate voltage after annealing). This indicates a downward shift of the Fermi level in the conduction band toward the lower DOS region (Figure 4f). With fewer carriers available in the low DOS region of the channel for the trapping/detrapping process, electric field sensitivity diminishes after annealing. A similar observation can also be made when comparing the sensitivity of a MoS_2 device with that of a graphene device. Figure 4e compares the electric field sensitivity of a single-layer MoS_2 device to that of a single-layer graphene device. The error bar is the standard deviation and the dot is the mean electric field sensitivity. MoS_2 device shows a much higher sensitivity than the graphene device for the same magnitude of the electric field. This can also be explained by the difference in the DOS at the Fermi level for both materials, as shown in Figure 4f. Graphene, whose Fermi level is around the CNP, has a much smaller DOS than MoS_2, whose Fermi level is around the conduction band edge for an n-type channel. This drastic difference in the DOS is translated into sensitivity, as it is dependent on the number of carriers available at the Fermi level.

CONCLUSIONS

In conclusion, we have demonstrated the use of a two-dimensional material, MoS_2, as an electric field sensor that can detect either polarity of the electric field. The sensitivity, defined as the percentage change in drain current under the electric field, has a linear dependence on the magnitude of the electric field. We have also shown that the sensitivity decreases with the thickness of the MoS_2 channel, with the single-layer device showing the highest sensitivity for the same magnitude of the electric field. In addition, we also compared the electric field sensitivity of the MoS_2 device to that of a graphene device and found that the former is much more sensitive than the latter.

AUTHOR INFORMATION

Corresponding Author

Afsal Kareekunnan − *School of Materials Science, Japan Advanced Institute of Science and Technology, Nomi 923-1292, Japan;* orcid.org/0000-0001-9008-3986; Email: afsal@jaist.ac.jp

Authors

Mohammad Razzakul Islam − *School of Materials Science, Japan Advanced Institute of Science and Technology, Nomi 923-1292, Japan*

Jiali Hu − *School of Materials Science, Japan Advanced Institute of Science and Technology, Nomi 923-1292, Japan*

Akihiro Kuki − *School of Materials Science, Japan Advanced Institute of Science and Technology, Nomi 923-1292, Japan*

https://doi.org/10.1021/acsomega.4c03350
ACS Omega 2024, 9, 29751−29755

Takeshi Kudo − *OTOWA ELECTRIC CO., LTD., Shioe Amagasaki 661-0976 Hyogo, Japan*
Takeshi Maruyama − *OTOWA ELECTRIC CO., LTD., Shioe Amagasaki 661-0976 Hyogo, Japan*
Atsushi Nishizaki − *OTOWA ELECTRIC CO., LTD., Shioe Amagasaki 661-0976 Hyogo, Japan*
Yuki Tokita − *OTOWA ELECTRIC CO., LTD., Shioe Amagasaki 661-0976 Hyogo, Japan*
Masashi Akabori − *School of Materials Science, Japan Advanced Institute of Science and Technology, Nomi 923-1292, Japan;* orcid.org/0000-0001-6346-3676
Hiroshi Mizuta − *School of Materials Science, Japan Advanced Institute of Science and Technology, Nomi 923-1292, Japan; School of Electronics and Computer Science, University of Southampton, Southampton SO17 1BJ, U.K.*

Complete contact information is available at: https://pubs.acs.org/10.1021/acsomega.4c03350

Author Contributions

‖M.R.I. and J.H. have contributed equally to this work.

Notes

The authors declare no competing financial interest.

■ ACKNOWLEDGMENTS

This research was supported by the research grants from OTOWA ELECTRIC CO., LTD., the Earth Inclusive Sensing Empathizing with Silent Voices (EISESiV) consortium, and the grant-in-Aid for Scientific Research (A) no. 23H00256 from the Japan Society for the Promotion of Science (JSPS).

■ REFERENCES

(1) Hill, E. W.; Vijayaragahvan, A.; Novoselov, K. Graphene Sensors. *IEEE Sens. J.* **2011**, *11*, 3161−3170.
(2) Novoselov, K. S.; Fal′ko, V. I.; Colombo, L.; Gellert, P. R.; Schwab, M. G.; Kim, K. A roadmap for graphene. *Nature* **2012**, *490*, 192−200.
(3) Kostarelos, K.; Novoselov, K. S. Graphene devices for life. *Nat. Nanotechnol.* **2014**, *9*, 744−745.
(4) Yu, X.; Cheng, H.; Zhang, M.; Zhao, Y.; Qu, L.; Shi, G. Graphene-based smart materials. *Nat. Rev. Mater.* **2017**, *2*, 17046.
(5) Wang, W.; Du, R.; Zafar, A.; He, L.; Zhao, W.; Chen, Y.; Lu, J.; Ni, Z. High-Performance Graphene-Based Electrostatic Field Sensor. *IEEE Electron Device Lett.* **2017**, *38*, 1136−1138.
(6) Kareekunnan, A.; Agari, T.; Hammam, A. M. M.; Kudo, T.; Maruyama, T.; Mizuta, H.; Muruganathan, M. Revisiting the mechanism of electric field sensing in graphene devices. *ACS Omega* **2021**, *6*, 34086−34091.
(7) Kareekunnan, A.; Agari, T.; Kudo, T.; Niwa, S.; Abe, Y.; Maruyama, T.; Mizuta, H.; Muruganathan, M. Graphene electric field sensor for large scale lightning detection network. *AIP Adv.* **2022**, *12*, 095209.
(8) Afsal, K.; Agari, T.; Kudo, T.; Maruyama, T.; Mizuta, H.; Muruganathan, M. Enhancement of Electric Field Sensitivity in Graphene for Early Lightning Prediction. *IEEE Explore Silicon Nanoelectronics Workshop (SNW)*, 2021; Vol. *1*−*2*.
(9) Novoselov, K. S.; Geim, A. K.; Morozov, S. V.; Jiang, D.; Zhang, Y.; Dubonos, S. V.; Grigorieva, I. V.; Firsov, A. A. Electric Field Effect in Atomically Thin Carbon Films. *Science* **2004**, *306*, 666−669.
(10) Novoselov, K. S.; Geim, A. K.; Morozov, S. V.; Jiang, D.; Katsnelson, M. I.; Grigorieva, I. V.; Dubonos, S. V.; Firsov, A. A. Two-dimensional gas of massless Dirac fermions in graphene. *Nature* **2005**, *438*, 197−200.
(11) Geim, A. K.; Novoselov, K. S. The rise of graphene. *Nat. Mater.* **2007**, *6*, 183−191.
(12) Schedin, F.; Geim, A. K.; Morozov, S. V.; Hill, E. W.; Blake, P.; Katsnelson, M. I.; Novoselov, K. S. Detection of individual gas molecules adsorbed on graphene. *Nat. Mater.* **2007**, *6*, 652−655.
(13) Mak, K. F.; Lee, C.; Hone, J.; Shan, J.; Heinz, T. F. Atomically Thin MoS_2: A New Direct-Gap Semiconductor. *Phys. Rev. Lett.* **2010**, *105*, 136805.
(14) Radisavljevic, B.; Radenovic, A.; Brivio, J.; Giacometti, V.; Kis, A. Single-layer MoS_2 transistors. *Nat. Nanotechnol.* **2011**, *6*, 147−150.
(15) Baik, S. S.; Im, S.; Choi, H. J. Work Function Tuning in Two-Dimensional MoS_2 Field-Effect-Transistors with Graphene and Titanium Source-Drain Contacts. *Sci. Rep.* **2017**, *7*, 45546.
(16) Britnell, L.; Ribeiro, R. M.; Eckmann, A.; Jalil, R.; Belle, B. D.; Mishchenko, A.; Kim, Y.-J.; Gorbachev, R. V.; Georgiou, T.; Morozov, S. V.; Grigorenko, A. N.; Geim, A. K.; Casiraghi, C.; Neto, A. H. C.; Novoselov, K. S. Strong Light-Matter Interactions in Heterostructures of Atomically Thin Films. *Science* **2013**, *340*, 1311−1314.
(17) Lee, C.; Yan, H.; Brus, L. E.; Heinz, T. F.; Hone, J.; Ryu, S. Anomalous Lattice Vibrations of Single- and Few-Layer MoS_2. *ACS Nano* **2010**, *4*, 2695−2700.
(18) Li, H.; Zhang, Q.; Yap, C. C. R.; Tay, B. K.; Edwin, T. H. T.; Olivier, A.; Baillargeat, D. From Bulk to Monolayer MoS_2: Evolution of Raman Scattering. *Adv. Funct. Mater.* **2012**, *22*, 1385−1390.
(19) Namgung, S. D.; Yang, S.; Park, K.; Cho, A. J.; Kim, H.; Kwon, J. Y. Influence of post-annealing on the off current of MoS_2 field-effect transistors. *Nanoscale Res. Lett.* **2015**, *10*, 62.
(20) Giannazzo, F.; Fisichella, G.; Piazza, A.; Di Franco, S.; Greco, G.; Agnello, S.; Roccaforte, F. Effect of temperature−bias annealing on the hysteresis and subthreshold behavior of multilayer MoS_2 transistors. *Phys. Status Solidi RRL* **2016**, *10*, 797−801.
(21) Ji, H.; Joo, M. K.; Yi, H.; Choi, H.; Gul, H. Z.; Ghimire, M. K.; Lim, S. C. Tunable Mobility in Double-Gated $MoTe_2$ Field-Effect Transistor: Effect of Coulomb Screening and Trap Sites. *ACS Appl. Mater. Interfaces* **2017**, *9*, 29185−29192.
(22) Bandyopadhyay, A. S.; Saenz, G. A.; Kaul, A. B. Role of metal contacts and effect of annealing in high performance 2D WSe_2 field-effect transistors. *Surf. Coat. Technol.* **2020**, *381*, 125084.
(23) Ghatak, S.; Pal, A. N.; Ghosh, A. Nature of Electronic States in Atomically Thin MoS_2 Field-Effect Transistors. *ACS Nano* **2011**, *5*, 7707−7712.
(24) Li, S. L.; Wakabayashi, K.; Xu, Y.; Nakaharai, S.; Komatsu, K.; Li, W. W.; Lin, Y. F.; Aparecido-Ferreira, A.; Tsukagoshi, K. Thickness-Dependent Interfacial Coulomb Scattering in Atomically Thin Field-Effect Transistors. *Nano Lett.* **2013**, *13*, 3546−3552.
(25) Li, S. L.; Komatsu, K.; Nakaharai, S.; Lin, Y. F.; Yamamoto, M.; Duan, X.; Tsukagoshi, K. Thickness Scaling Effect on Interfacial Barrier and Electrical Contact to Two-Dimensional MoS_2 Layers. *ACS Nano* **2014**, *8*, 12836−12842.
(26) Das, S.; Appenzeller, J. Screening and interlayer coupling in multilayer MoS_2. *Phys. Status Solidi RRL* **2013**, *7*, 268−273.
(27) Das, S.; Appenzeller, J. Where Does the Current Flow in Two-Dimensional Layered Systems? *Nano Lett.* **2013**, *13*, 3396−3402.
(28) Das, S.; Chen, H. Y.; Penumatcha, A. V.; Appenzeller, J. High Performance Multilayer MoS_2 Transistors with Scandium Contacts. *Nano Lett.* **2013**, *13*, 100−105.